AMSE JOURNALS-AMSE IIETA publication-2017-Series: Modelling B; Vol. 86; N°4; pp 864-884
Submitted Oct. 2017; Revised Dec. 13, 2017, Accepted Dec. 30, 2017

MHD Heat and Mass Transfer on Stretching Sheet with Variable Fluid Properties in Porous Medium

*K. Swain, **S.K. Parida, **G.C. Dash

[*] Department of Mathematics, Radhakrishna Institute of Technology & Engineering, Bhubaneswar, 752057, India
[**] Department of Mathematics, Institute of Technical Education and Research, Siksha 'O' Anusandhan (Deemed to be University), Bhubaneswar-751030, India
(kharabela1983@gmail.com)

Abstract

An analysis is carried out on steady two dimensional stagnation point flow of an incompressible conducting viscous fluid with variable properties over a stretching surface embedded in a saturated porous medium. The flow model is subjected to (i) transverse magnetic field, (ii) variable viscosity and thermal conductivity, (iii) thermodiffusion (Soret effect), (iv) stretching of both plate and free stream (v) pressure gradient in the flow direction is considered non-zero. The Runge-Kutta fourth order method with a self corrective procedure i.e. shooting technique has been applied to solve the governing equations. An interesting result of the analysis is that inversion in formation of velocity boundary layer is due to reversal in stretching ratio. On the other hand, heat transfer leading to formation of thermal boundary layer is not affected significantly. Variable thermal conductivity enhances the temperature distribution. Increase in concentration difference and thermophoresis parameter gives rise to thinner solutal boundary layer. Further, it is remarked that heavier chemically reactive species enhance the rate of solutal transfer at the surface.

Keywords

MHD, Variable viscosity, Variable conductivity, Thermophoresis, Stretching sheet, Heat source.

1. Introduction

The exact solutions of two dimensional and three dimensional viscous flow near a stagnation point may be obtained from the consideration that at large distance from the stagnation point, the flow is essentially the same as that of the corresponding potential flow problem. Thus, the solution of this class of flow problem may be derived from the solution of the inviscid flow (potential flow) problem. Application of a transverse magnetic field fixed to the body should reduce the heat transfer at the stagnation point and increase the body's drag. Both these results are desirable for the protecting the vehicle reentering the atmosphere (Cramer and Pai [1]). The flow in the neighborhood of a stagnation point was first studied by Hiemenz [2]. Stagnation point flow is an important class of problem in hydrodynamics as because exact solution of Navier-Stokes equations is possible in such flow problems. Many authors such as Vajravelu [3], Sharma and Jat [4], Chaim [5] studied stagnation point flow in presence of internal dissipation. The objective of the present study is to account for the variable fluid properties such as viscosity and conductivity as the fluid properties are amenable to thermal and mass diffusion. Another striking feature of the study is to consider the effect of thermophoresis which causes small particles to be drifted from hot surface due to temperature gradient which is a common phenomenon in many industrial processes associated with mass transfer. The thermophoresis is an effective mass transfer mechanism in the chemical vapour deposition process used in fabrication of optical fiber. Goren [6] has studied thermophoretic effect on laminar flow over a horizontal flat plate. Shen [7] considered the thermophoretic deposition onto cold surfaces. Makinde et al. [8] have studied the effects of Brownian motion, thermophoresis and magnetic field on stagnation point flow and heat transfer due to nanofluid flow towards a stretching sheet. Further, Nadeem et al. [9] have studied a steady stagnation point flow with heat transfer of a second grade nanofluid on a stretching surface. They applied homotopy analysis method (HAM) to solve the resulting equations. Reddy [10] has studied the effect of thermophoresis, viscous dissipation and Joule heating on steady MHD flow over an inclined radiative isothermal permeable surface with variable thermal conductivity. Parida and Rout [11] have studied free convective flow with variable permeability with couple stress and heat source through porous medium. Muhaimin et al. [12] examined the effects of thermophoresis and chemical reaction on unsteady MHD mixed convective flow over a porous wedge considering temperature-dependent viscosity. Chen [13] has studied the MHD flow and heat transfer for two types of viscoelastic fluid over a stretching sheet with energy dissipation, internal heat source and thermal radiation. The governing equations are solved analytically using Kummer's functions. Nayak et.al [14] have studied steady MHD flow and heat transfer of a third grade fluid in wire coating analysis with temperature dependent viscosity. They have considered Reynold's and Vogel's model for variable viscosity. They have not considered the effect of thermophoresis in their study. The governing equations of the flow model due to inclusion of variable fluid properties and thermophoresis, the analytical solution seems to be difficult. Therefore, fourth order Runge-Kutta method with shooting technique has been applied to solve the governing equations. The study of flow through porous medium has many applications in physical, chemical and biological processes. The problem of MHD flow of an incompressible viscous electrically conducting fluid past a porous plate through a porous medium with uniform angular velocity about a non coincident parallel axis has been studied by Parida et al. [15]. Parida and Dash [16] have studied the dusty fluid flow through a porous medium under the influence of transverse magnetic field in presence of heat source. Panda et al. [17] have studied the three dimensional MHD free convective flow with heat and mass transfer through a porous medium with periodic permeability. Sahoo et al. [18] have studied the unsteady two dimensional MHD flow and heat transfer of an elastico-viscous liquid past an infinite hot vertical porous surface bounded by porous medium with source/sink. Further, the hydro-magnetic flow and heat transfer through porous medium in a elastico-viscous fluid over a porous plate in the slip flow regime has been studied by Panda et al. [19].

The present investigation is a renewed interest over the works of Rahman [20], El-Sayed and Elgazery [21], Sharma and Singh [22]. Rahman [20] in his study suggested a locally similar solution for hydromagnetic and thermal slip flow over a flat plate with variable fluid properties and convective bounding surface condition. He has restricted his study to the variable viscosity and conductivity without considering the variation of solutal concentration in the process of mass transfer of diffusing species. El-Sayed and Elgazery [21] have studied the problem considering the variable fluid properties and thermophoresis effect in mass diffusion process but the problem does not account for the stretching of bounding surface, instead, accounts for the variable suction at the surface. Sharma and Singh [22] have studied the effects of variable thermal conductivity keeping the viscosity of the fluid constant; though viscosity property is amenable to thermal property of the fluid. Moreover, they have not considered mass transfer as well as diffusion of thermo effect in their studies.

Thus, the novelty of the present study involves interaction of electromagnetic force with variable material properties of the fluid related to three boundary layers such as velocity, thermal and solutal. Further, the flow is set to pass through a saturated porous medium which resists the flow in the boundary layer under study. Moreover, heat transfer equation is associated with volumetric heat source and the solutal concentration variation is modified by the inclusion of diffusion thermo effect. The results of the present numerical method are validated by comparing with the results reported earlier. The most important application of MFD is the generation of electrical power with the flow of an electrically conducting fluid through a transverse magnetic field. For generating power on large scale in stationary plants with large magnetic fields (about 5 Weber/m^2) cryogenic and super conducting magnets are required to produce these very large magnetic fields. Generation of MFD power on a small scale is of interest for space application [1].

2. Formulation of the Problem

Consider the two dimensional viscous flow of an incompressible electrically conducting fluid with a variable viscosity and thermal conductivity near a stagnation point on a non-conducting stretching sheet $y = 0$, the flow being in the region $y > 0$. The velocity and temperature of the stretching sheet are set to uw(x) and T_w.

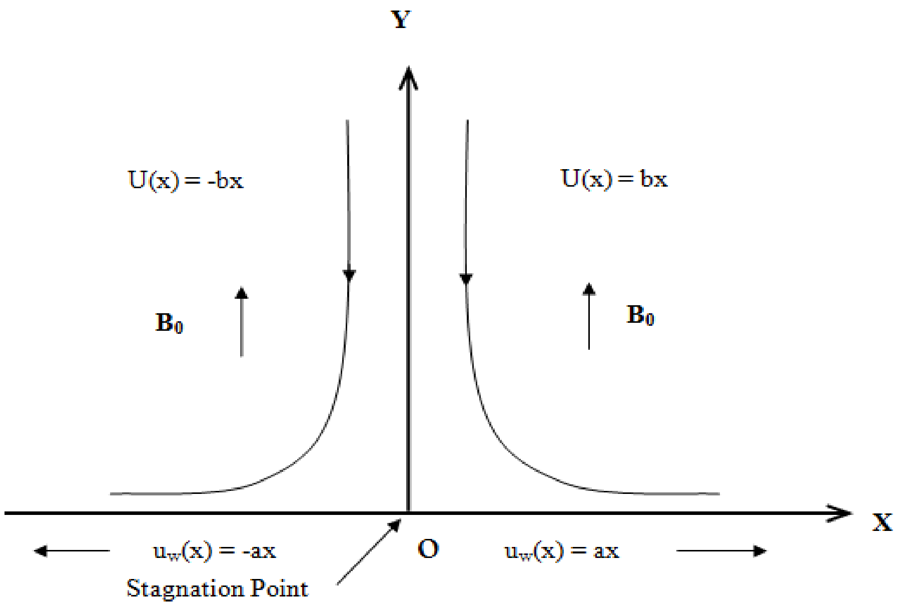

Fig. 1. A Sketch of the Physical Problem

The governing equations of continuity, momentum, energy and concentration under the influence of externally imposed transverse magnetic field (magnetic field fixed to the plate), variable thermal conductivity with thermophoresis in the boundary layer flow composed with porous medium with permeability $\left(Kp^*\right)$ in the presence of transverse magnetic field with strength B_0 following Rahman [20], Sharma and Singh [22] are given by

$$\frac{\partial u}{\partial x}+\frac{\partial v}{\partial y}=0 \tag{1}$$

$$u\frac{\partial u}{\partial x}+v\frac{\partial u}{\partial y}=-\frac{1}{\rho}\frac{\partial p}{\partial x}+\frac{1}{\rho}\frac{\partial}{\partial y}\left(\mu\frac{\partial u}{\partial y}\right)-\frac{\sigma B_0{}^2}{\rho}u-\frac{\mu}{\rho Kp^*}u \tag{2}$$

$$\rho C_p\left(u\frac{\partial T}{\partial x}+v\frac{\partial T}{\partial y}\right)=\frac{\partial}{\partial y}\left(k^*\frac{\partial T}{\partial y}\right)+Q\left(T-T_\infty\right) \tag{3}$$

$$u\frac{\partial C}{\partial x}+v\frac{\partial C}{\partial y}=D\frac{\partial^2 C}{\partial y^2}-\frac{\partial}{\partial y}\left(V_T C\right) \tag{4}$$

where V_T, the thermophoretic velocity as suggested by Talbot et.al [23] is given by

$$V_T=-\frac{t_p\mu}{\rho T_f}\frac{\partial T}{\partial y}$$

where $\frac{t_p\mu}{\rho T_f}$ contributes to thermophoretic diffusivity, t_p is the thermophoretic coefficient, $0.2<t_p<1.2$ indicated by Batchelor [24].

The LHS of binary diffusion equation (4) has two terms. The first term describes the diffusion due to concentration gradient. It is known as Fick's diffusion law and corresponds the Fourier heat conduction law in the thermal boundary layer. The binary diffusion coefficient, D is a physical property. The second term describes the thermodiffusion (also called Soret effect). This gives rise to an additive mass transfer because of the temperature gradient. Therefore, there is a coupling effect between heat transfer and mass transfer. The present analysis is carried out so that the dimensionless thermal diffusion coefficient τ is as far as possible independent of the concentration but function of y-coordinate, where as the binary diffusion coefficient D is constant. We have avoided further coupling here i.e. diffusion thermo effect or Dufour effect Sparrow et al [25] assuming the level of species concentration is low. In many cases the coupling effects are small enough to be neglected compared to the effects of diffusion or heat conduction. However, there are exceptions such as the thermodiffusion is used in separating isotopes and the diffusion thermo effect is used in mixtures of gases with very different molar masses [26].

In the free stream $u=U(x)$ represents potential flow and the equation (2) reduces to

$$U\frac{\partial U}{\partial x}+\frac{\sigma B_0^{\,2}}{\rho}U+\frac{\mu}{Kp^*}U=-\frac{1}{\rho}\frac{\partial p}{\partial x}$$

(5)

Eliminating $\frac{\partial p}{\partial x}$, the equations (2) and (5), we obtain

$$u\frac{\partial u}{\partial x}+v\frac{\partial u}{\partial y}=U\frac{dU}{dx}+\frac{1}{\rho}\frac{\partial}{\partial y}\left(\mu\frac{\partial u}{\partial y}\right)-\frac{\sigma B_0^{\,2}}{\rho}(u-U)-\frac{\mu}{\rho Kp^*}(u-U) \tag{6}$$

The boundary conditions are

$$\left.\begin{array}{l} y=0: \quad u=u_w(x)=ax, \;\; v=0, \;\; T=T_w, \;\; \mathrm{C}=\mathrm{C}_\mathrm{w} \\ y\to\infty: \quad u=U(x)=bx, \;\; T=T_\infty, \;\; C=C_\infty \end{array}\right\} \tag{7}$$

We introduce the stream function $\psi(x,y)$ as $u=\frac{\partial\psi}{\partial y}$ and $v=-\frac{\partial\psi}{\partial x}$ and similarity variables $\eta=\left(\frac{a}{\upsilon}\right)^{1/2}y$ and $\psi(x,y)=(a\upsilon)^{1/2}xf(\eta)$

Following Ling and Dybbs [27] the temperature dependent viscosity as

$$\frac{1}{\mu}=\frac{1}{\mu_\infty}\left[1+\gamma(T-T_\infty)\right] \tag{8}$$

where γ is the thermal property of the fluid. Hence equation (8) can be rewritten as

$$\frac{1}{\mu}=\frac{\gamma}{\mu_\infty}(T-T_r) \tag{9}$$

where $T_r=T_\infty-\frac{1}{\gamma}$

The dimensionless temperature $\theta=\frac{T-T_r}{T_w-T_\infty}+\theta_r$ (10)

where $\theta_r=\frac{T_r-T_\infty}{T_w-T_\infty}=-\frac{1}{\gamma(T_w-T_\infty)}$

Using (10), equation (9) becomes

$$\mu=\mu_\infty\left(\frac{\theta_r}{\theta_r-\theta}\right) \tag{11}$$

Moreover, Arunachalam and Rajappa [28] and Chaim [29], considered the variable thermal conductivity k^* as

$$k^* = k(1+\varepsilon\theta) \tag{12}$$

Using the non-dimensional variables and parameters

$$\theta = \frac{T - T_\infty}{T_w - T_\infty},\ \ \varphi = \frac{C - C_\infty}{C_w - C_\infty},\ \ Nc = \frac{C_\infty}{C_w - C_\infty},\ \ M = \left(\frac{\sigma B_0^2}{\rho a}\right), Kp = \frac{\upsilon}{Kp^* a}$$
$$\Pr = \frac{\mu C_p}{k},\ \ Sc = \frac{\upsilon}{D},\ \ \lambda = \frac{b}{a},\ \ S = \frac{Q}{a\rho C_p},\ \ \tau = -\frac{t_p\left(T_w - T_\infty\right)}{T_f} \tag{13}$$

we get the following non dimensional equations and corresponding boundary conditions

$$\frac{\theta_r}{\theta_r - \theta} f''' + \frac{\theta_r}{\left(\theta_r - \theta\right)^2} f''\theta' + ff'' - \left(f'\right)^2 - \left(M + Kp\right)\left(f' - \lambda\right) + \lambda^2 = 0$$

(14)

$$\left(1 + \varepsilon\theta\right)\theta'' + \varepsilon\left(\theta'\right)^2 + \Pr\theta' f + \Pr S\theta = 0$$

(15)

$$\phi'' + Scf\phi' - \tau Sc\frac{\theta_r}{\theta_r - \theta}\left[\theta'' + \theta'\phi' + Nc\left\{\theta'' + \frac{\left(\theta'\right)^2}{\theta_r - \theta}\right\}\right] = 0 \tag{16}$$

$$\left.\begin{array}{l} f\left(0\right) = 0,\ f'\left(0\right) = 1,\ \ \theta\left(0\right) = 1,\ \ \varphi\left(0\right) = 1 \\ f'\left(\infty\right) = \lambda,\ \ \theta\left(\infty\right) = 0,\ \ \varphi\left(\infty\right) = 0 \end{array}\right\} \tag{17}$$

The parameters of physical interest such as skin-friction coefficient, Nusselt number and Sherwood number are

$$C_f = \frac{\tau_w}{\rho_\infty a\left(a\upsilon\right)^{1/2}}, Nu = \frac{xq_w}{k\left(T_w - T_\infty\right)},\ \text{and}\ \ Sh = \frac{xq_m}{D\left(C_w - C_\infty\right)}$$

(18)

$$\text{where}\ \tau_w = \mu\left(\frac{\partial u}{\partial y}\right)_{y=0}, q_w = -k^*\left(\frac{\partial T}{\partial y}\right)_{y=0},\ \text{and}\ \ q_m = -k^*\left(\frac{\partial C}{\partial y}\right)_{y=0} \tag{19}$$

In non-dimensional form equation (18) is given by

$$C_f = \left(\frac{\theta_r}{\theta_r - \theta\left(0\right)}\right)\frac{1}{\sqrt{\mathrm{Re}_x}} f''\left(0\right), Nu = -\left(1 + \varepsilon\theta\right)\sqrt{\mathrm{Re}_x}\,\theta'\left(0\right),\ \text{and}\ Sh = -\sqrt{\mathrm{Re}_x}\,\phi'\left(0\right) \tag{20}$$

where $\mathrm{Re}_x = ax^2/\upsilon$ is the local Reynolds number.

3. Results and Discussion

The equations (14), (15) and (16) are coupled and nonlinear equations. The nonlinear equations with boundary conditions (17) forms a two-point boundary value problem (BVP) and are solved using the fourth order Runge-Kutta method with shooting technique. In order to test the consistency of the solution, three different step sizes such as; $\Delta\eta = 0.004$, $\Delta\eta = 0.002$ and $\Delta\eta = 0.001$ are used in the process of computation. It is observed that $\Delta\eta = 0.001$ provides sufficiently accurate (error less than 10^{-6}) results. In order to compare the results of the present study with the earlier works, the shear stress $f''(0)$ at the stretching surface this has been presented in table 1. From equation (14) and corresponding boundary conditions (17), the following earlier works are derived as special cases.

(i) $\theta_r \to \infty$, Sharma and Singh [22].

(ii) $\theta_r \to \infty, \mathrm{M} = 0, Kp = 0$, Pop et al. [30].

(iii) $\theta_r \to \infty, \mathrm{M} = 0, Kp = 0, S = 0, b = 0$, Chiam [29].

(iv) $\theta_r \to \infty, \mathrm{M} = 0, Kp = 0, S = 0, b = 0, \varepsilon = 0$, Mahapatra and Gupta [31]

It is observed from Table 1 that the present work is in good agreement with the previous works. Further, it shows that $f''(0)$ changes sign, when λ shifts from $\lambda < 1$ to $\lambda > 1$; hence the relative rates of stretching of the plate and free stream may be pre assigned as per the modeling requirement.

Table 1. Skin friction, $f''(0)$ for different values of λ, the ratio of stretching rates

λ	$f''(0)$			
	Mahapatra and Gupta [31]	Pop et al. [30]	Sharma and Singh [22]	Present Study
0.1	-0.9694	-0.9694	-0.969386	-0.96965625
0.2	-0.9181	-0.9181	-0.9181069	-0.91816450
0.5	-0.6673	-0.6673	-0.667263	-0.66726432
2.0	2.0175	2.0174	2.01749079	2.01750252
3.0	4.7293	4.7290	4.72922695	4.72928082

The table 2 presents dimensionless heat flux at the surface $-\theta'(0)$ for $M = 0,\ Kp = 0,\ \lambda = 0,\ S = 0,\ \theta_r \to \infty,\ \Pr = 0.023$. It is found that values of $-\theta'(0)$ agree with the results obtained by Chaim [29] and Sharma and Singh [22] with differences shown in the table. It is remarked that the difference increases with the higher value of thermal conductivity parameter ε. Therefore, it is concluded that small variation in thermal conductivity parameter ε desirable.

Tab. 2. Values of $-\theta'(0)$ for Different Values of Thermal Conductivity, ε

ε	Chiam [29]	Sharma and Singh [22]	Present Study
0.0	0.224886	0.22489	0.22488274
0.05	0.214397	0.21440	0.21932532
0.1	0.204844	0.20485	0.21426800

Table 3 presents the rate of heat transfer (Nusselt number) at the plate for different values of stretching parameter λ . It increases with greater stretching rate steadily irrespective of $\lambda > 1$ or $\lambda < 1$. Thus, it is remarked that rate of heat transfer is not affected much irrespective of $\lambda > 1$ or $\lambda < 1$. It was also supported by the previous authors Sharma and Singh [22], Pop et al. [30], Mahapatra and Gupta [31].

Tab. 3. Values of $-\theta'(0)$ for Different Values of λ

λ	$-\theta'(0)$			
	Pop et al. [30]	Mahapatra and Gupta [31]	Sharma and Singh [22]	Present Study
0.1	0.081	0.081	0.081245	0.08229665
0.5	0.135	0.136	0.135571	0.13557159
2.0	0.241	0.241	0.241025	0.24102456

From table 4, it is seen that $f''(0)$ increases with magnetic field strength and stretching rate being $\lambda > 1$ but decreases with $\lambda < 1$. The decrease in skin friction gives rise to an asymptotic fall in velocity. Magnetic field does not produce flow separation or reverse flow Cramer and Pai [1]. Moreover, the increase in temperature due to permeability parameter may be attributed to the resistance offered by the porous medium to the flow. Thus, the positive and negative values of skin friction indicate the formation of boundary layers and inverted boundary layer for $\lambda > 1$ and $\lambda < 1$ respectively. It is further concluded that increase in greater magnetic field strength, enhances $f''(0)$ slightly, on the other hand higher stretching ratio λ contribute significantly. Therefore, greater rate of free stream stretching is not favorable for the reduction of skin friction.

Tab. 4. Values of $f''(0)$ for Different Values of λ and M.

λ	$f''(0)$				
	M=0.0	M=0.1	M=0.5	M=1.0	M=1.5
0.1	-0.96965625	-0.97376816	-1.06799955	-1.32111841	-1.66020814
0.2	-0.91816450	-0.92158975	-1.00049272	-1.21562579	-1.50850048
0.5	-0.66726432	-0.66910298	-0.71189178	-0.83212616	-1.00168334
2.0	2.01750252	2.019944307	2.07772440	2.24910348	2.50962337
3.0	4.72928082	4.733453542	4.83256039	5.13037885	5.59263544

Table 5 shows that the rate of heat transfer decreases with an increase in the values of M, ε and Pr in the presence of volumetric heat source but increases in the presence of sink as the presence of sink absorbs heat and hence to compensate the loss, rate of heat transfer at the bounding surface increases.

Tab. 5. Values of Rate of Heat Transfer for Different Values of λ, ε, M, θ_r, Pr, S.

M	ε	λ	Pr	S	$-\theta'(0)$
0	0	0.1	0.023	0	0.049828
0	0.1	0.1	0.023	0	0.046372
0.5	0.1	0.1	0.023	0.1	0.015002
0.5	0.1	0.1	0.01	0.1	0.006570
0.5	0.1	0.1	0.01	-0.1	0.043692

Table 6 displays the rate of mass transfer i.e. Sherwood number. It is to note that an increase in thermophoretic parameter (τ) and Schmidt number (Sc), leads to increase the rate of mass whereas, a reverse effect is observed in case of variable viscosity parameter (θ_r) and heat source strength. Thus, it is concluded that heavier species combined with thermophoresis enhances the mass transfer rate at the plate but variable viscosity and heat source affects adversely.

Tab. 6. Values of Rate of Mass Transfer for Different Values of θ_r, τ, Sc, S.

θ_r	τ	Sc	S	$-\phi'(0)$
5	0.0	0.22	0.1	0.292099
5	0.5	0.22	0.1	0.313355
-5	0.5	0.22	0.1	0.2929937

5	0.5	0.5	0.1	0.4480516
2	0.5	0.5	0.1	0.5291917
2	0.5	0.5	0.01	0.5349787
2	0.5	0.5	-0.01	0.5362359

From figure 2, it is remarked that inversion of boundary layer occurs for $\lambda > 1$ and $\lambda < 1$ i.e. free stream stretching velocity is greater than plate stretching and vice-versa. Moreover, it is noticed that for $\lambda = 1$, there is no formation of boundary layer since stretching velocity of the plate is equal to free stream velocity and hence, no momentum transfer occurs. The effect of higher value of magnetic parameter (M) is significant and the profiles are distinct.

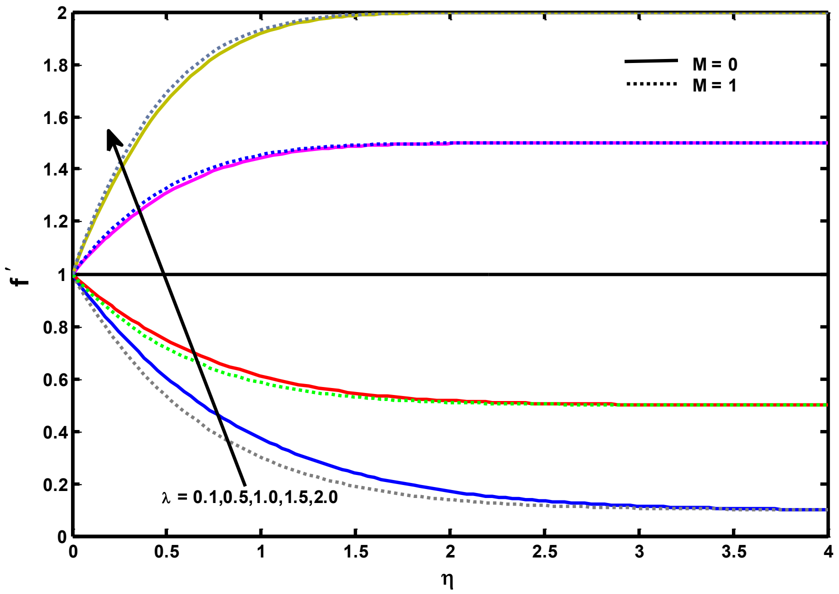

Fig. 2. Velocity Profile for Various Values of λ When M = 0.0, 1.0

Figure 3 shows that an increase in porosity parameter (Kp) leads to increase the velocity at all the points in the boundary layer for $\lambda > 1$.

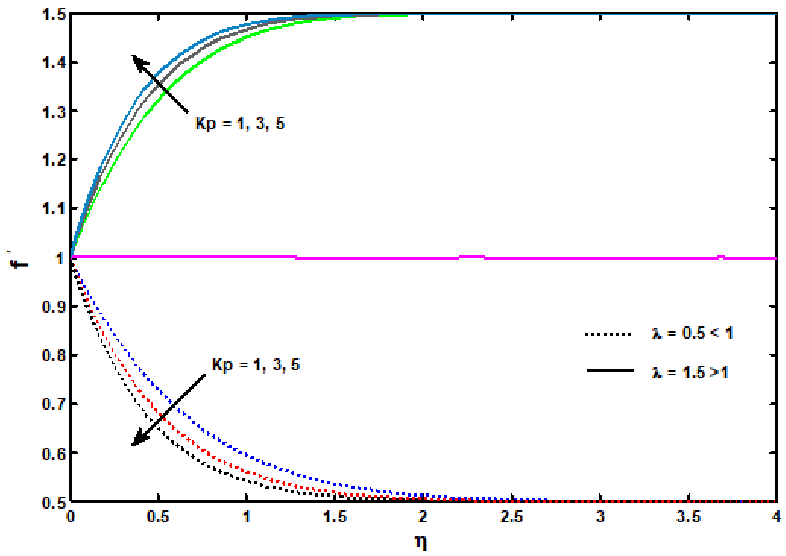

Fig. 3. Velocity Profile for Various Values of Kp When $\lambda < 1$ and $\lambda > 1$

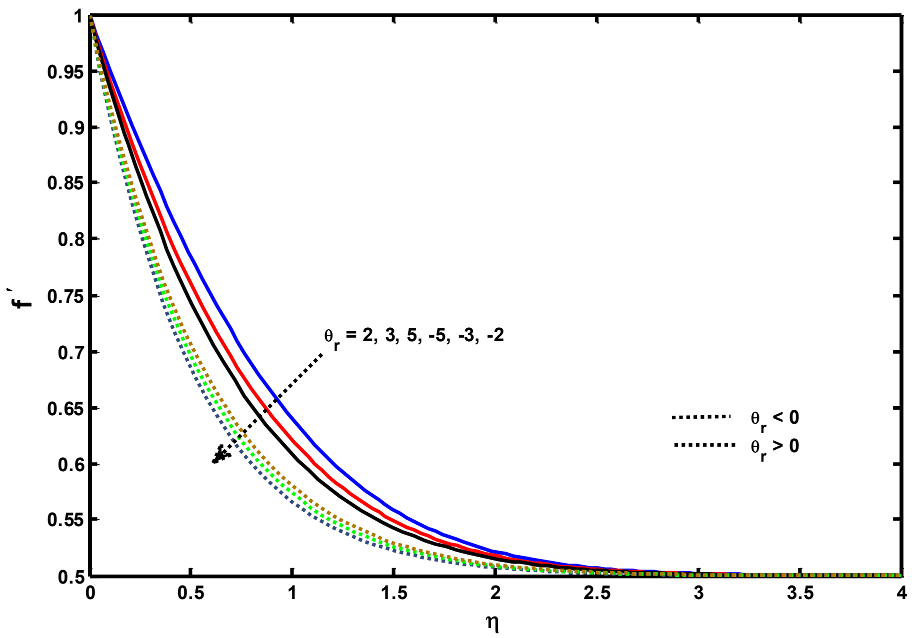

Fig. 4. Velocity Profile for Various Values of θ_r

Figure 4 exhibits the effect of variable viscosity parameter (θ_r) on velocity distribution. It is observed that an increase in viscosity parameter (θ_r) reduces the velocity for both $\theta_r > 0$ $(\theta_r = 2,3,5)$ and $\theta_r < 0$ $(\theta_r = -5,-3,-2)$. The variation is asymptotic in nature commensurate with ambient condition.

Figures 5 and 6 show that increase in magnetic parameter as well as porosity parameter enhance the temperature slightly. This further shows that temperature gets enhanced due to the presence of magnetic field.

Figure 7 shows that an increase in λ leads to decrease the temperature distribution. One striking feature of the temperature distribution is that temperature distribution does not show anomalous behavior depending upon stretching ratio $\lambda < 1$ and $\lambda > 1$ as shown in velocity distribution (Figure 2) depicting inversion distribution resulting in formation of inverted boundary layer.

Figure 8 shows that the temperature distribution decreases with an increase in $\Pr$. The Prandtl number (Pr) signifies the ratio of momentum diffusivity to thermal diffusivity. Fluids with lower Prandtl number will posse higher thermal conductivity resulting thicker thermal boundary layer structure so that heat can diffuse from the sheet faster.

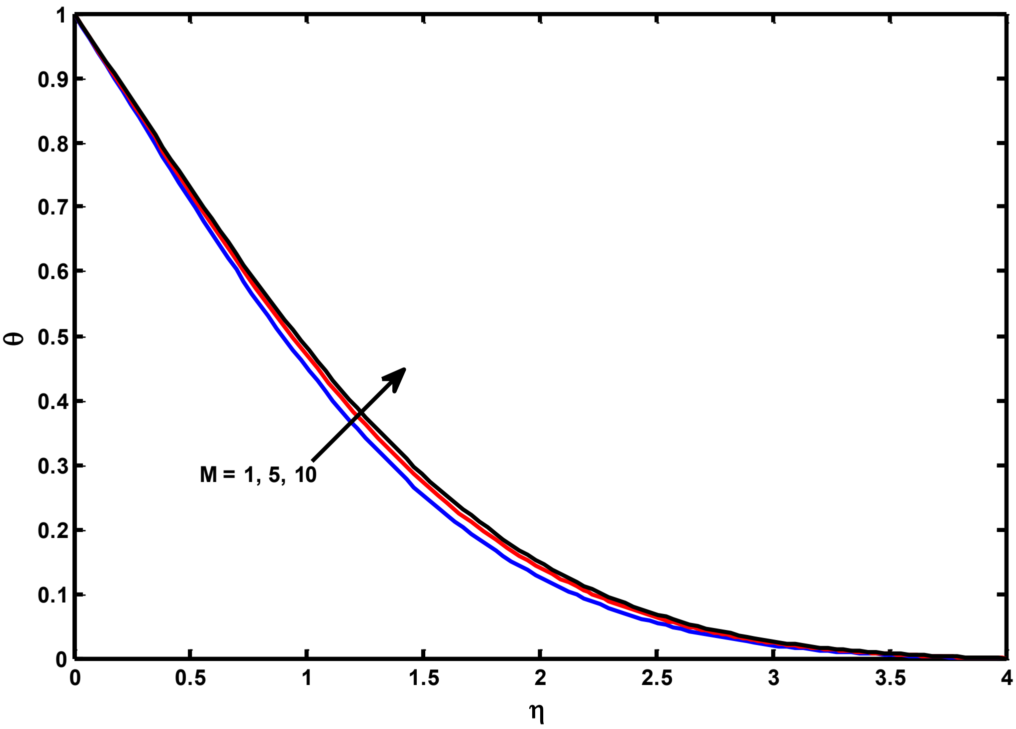

Fig. 5. Temperature Profile for Various Values of M

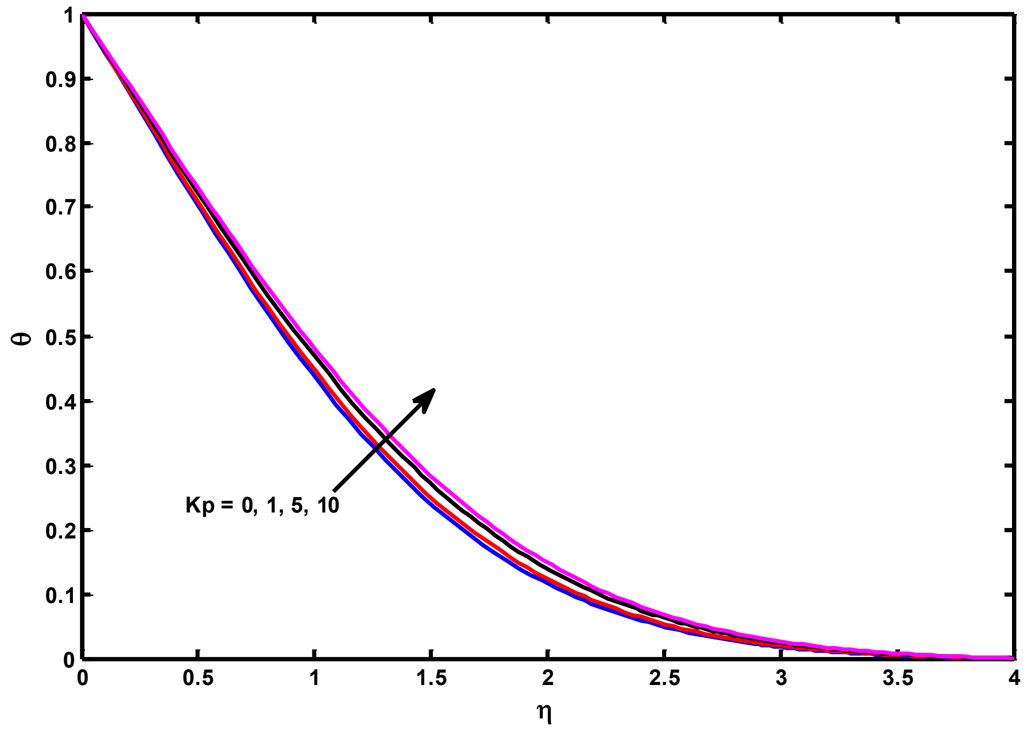

Fig. 6. Temperature Profile for Various Values of *Kp*

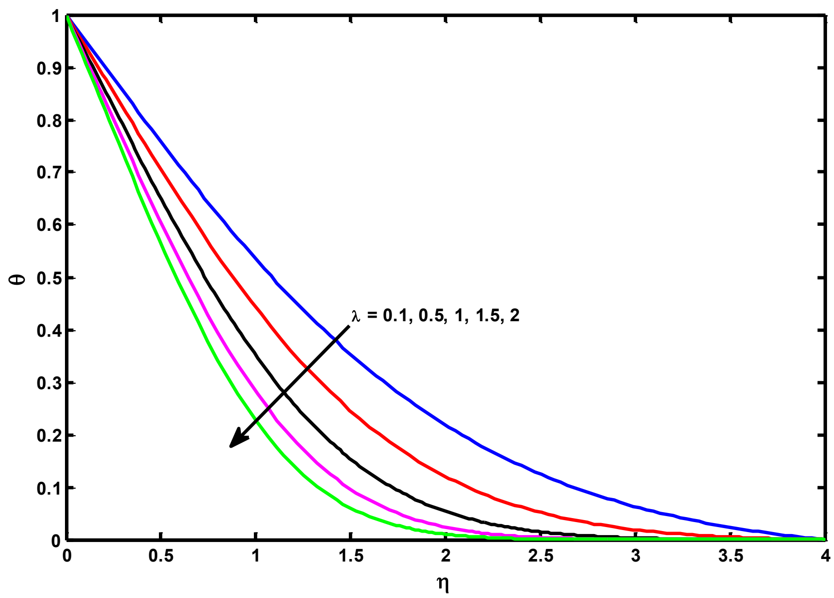

Fig. 7. Temperature Profile for Various Values of λ

Figure 9 shows that an increase in variable thermal conductivity parameter is favorable for rise in temperature. The case of constant thermal conductivity can be retrieved when $\varepsilon = 0$ which is evident from equation (12).

Figures 10, 11 and 12 show that heavier species i.e. higher value of *Sc* as well as *Nc* and τ give rise to thinner solutal boundary layer. Most importantly, the thermophoretic parameter is being affected by temperature difference between free stream and thermal boundary layer. The increase in difference of temperatures causes thinner solutal boundary layer.

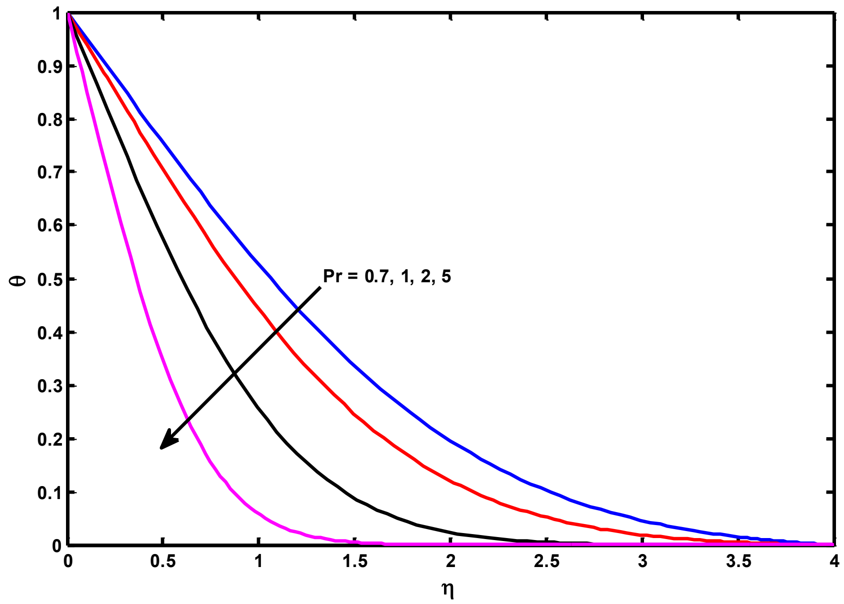

Fig. 8. Temperature Profile for Various Values of Pr

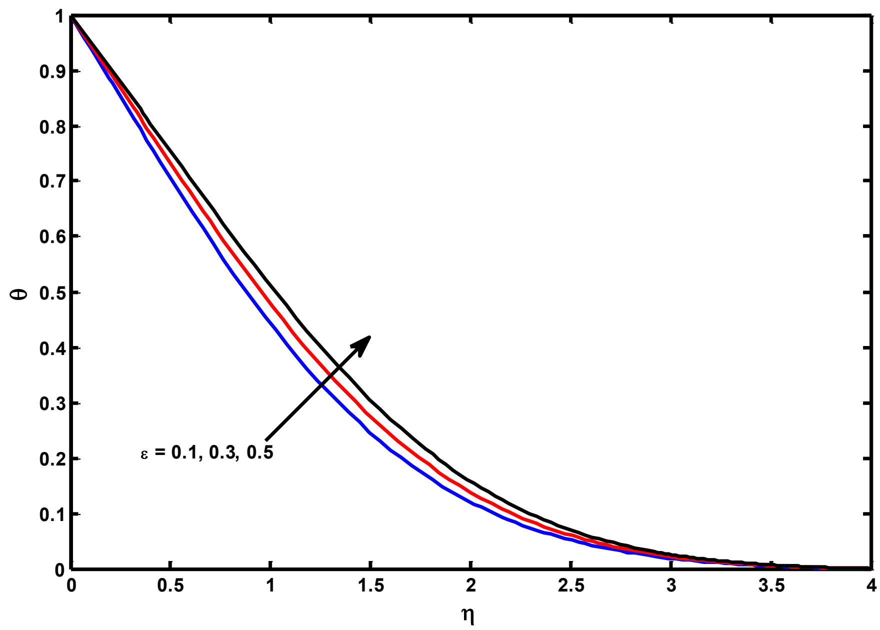

Figure 9. Temperature Profile for Various Values of ε

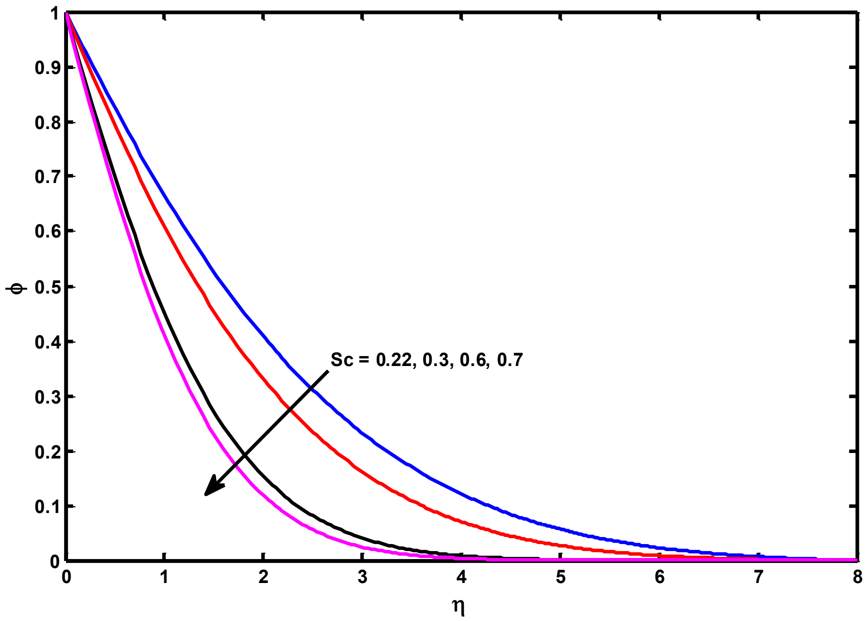

Fig. 10. Concentration Profile for Various Values of Sc

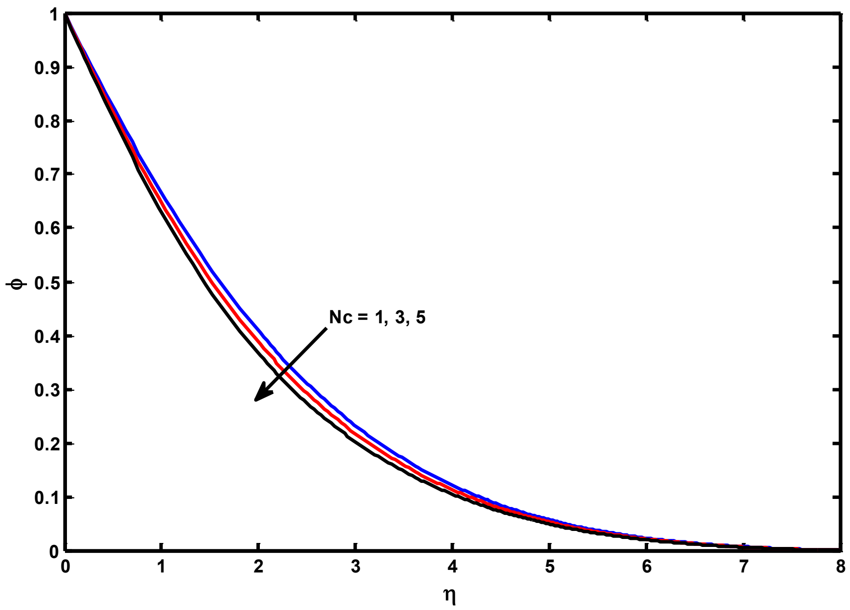

Fig. 11. Concentration Profile for Various Values of Nc

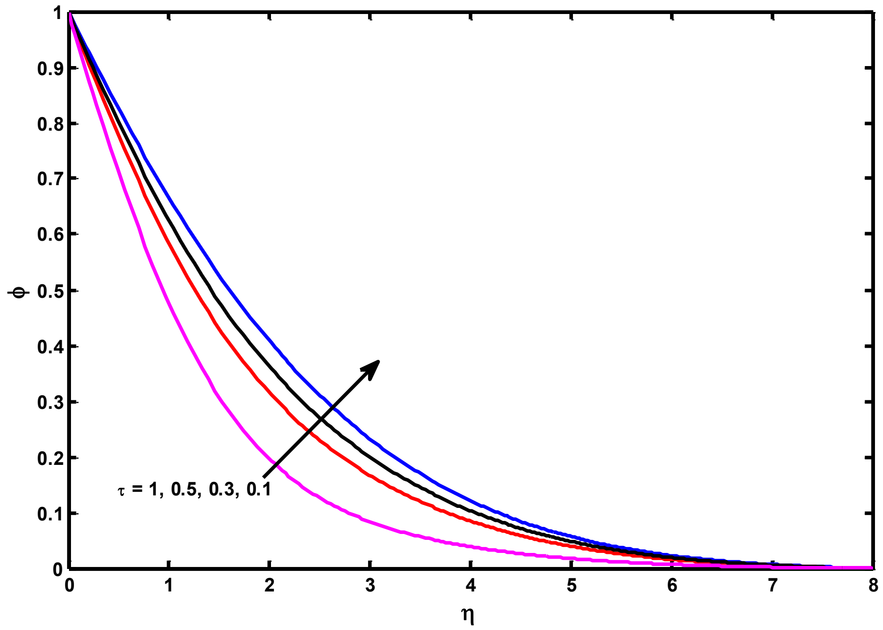

Fig. 12. Concentration Profile for Various Values of τ

Conclusions

From the present study following conclusions are drawn.

(i) A radical variation is marked in shearing stress at the plate due to variation in the ratio of rates of stretching of deformable surface to that of free stream (Table 1) but the variation is not so significant on the rate of heat transfer at the plate (Table 3) as because the momentum transport at the surface gets affected more than the transport of thermal energy.

(ii) Inversion in formation of velocity boundary layer occurs due to stretching ratio reversal.

(iii) Presence of porosity and magnetic field enhance the temperature distribution.

(iv) There is no inversion in the formation of thermal boundary layer. Thus, the reversal of stretching ratio fails to affect transport of thermal energy like momentum transport.

(v) Increase in concentration difference and thermophoresis is resulted in thinner solutal boundary layer.

References

1. R.Cramer Kenneth, S.I. Pai, Magnetic flow dynamics for engineering and applied physicists, 1973, Scripta Publishing Company, Washington D.C., p. 144.
2. K. Hiemanz, Die grenzschicht an einem in den gleich formigen flussigkeitsstrom eingetauchten geraden kreiszlinder, 1911, Dingl. Polytec. J. vol. 326, pp. 321-328.

3. K. Vajravelu, J. Nayfeh. Convective heat transfer at a stretching sheet, 1993, Acta Mechanica vol. 96, no. 1-4, pp. 47-54.
4. P.R. Sharma, R.N. Jat, Flow and heat transfer between two vertical plates under viscous fluid injection through porous plate, the other being stretching sheet, 1994, Indian J. Technology, India vol. XXXIII, pp. 21-30.
5. T.C. Chaim, Magnetohydrodynamic heat transfer over a non-isothermal stretching sheet, 1997, Acta Mechanica, vol. 122, no. 1-4, pp. 169-179.
6. S.L. Goren, Thermophoresis of aerosol particles in the laminar boundary layer on a flat plate, 1977, Journal of Colloid and Interface Science, vol. 61, no. 1, pp. 77-85.
7. C. Shen, Thermophoretic deposition of particles onto cold surfaces of bodies in two-dimensional and axisymmetric flows, 1989, Journal of Colloid and Interface Science, vol. 127, no. 1, pp. 104-115.
8. O.D. Makinde, W.A. Khan, Z.H. Khan, Buoyancy effects on MHD stagnation point flow and heat transfer of a nanofluid past a convectively heated stretching/shrinking sheet, 2013, International Journal of Heat and Mass Transfer, vol. 62, pp. 526-533.
9. S. Nadeem, R. Mehmood, N.S. Akbar, Non-orthogonal stagnation point flow of a nano non-Newtonian fluid towards a stretching surface with heat transfer, 2013, International Journal of Heat and Mass Transfer, vol. 57, pp. 579-589.
10. G.M. Reddy, Effects of thermophoresis, viscous dissipation and joule heating on steady MHD flow over an inclined radiative isothermal permeable surface with variable thermal conductivity, 2014, Journal of Applied Fluid Mechanics, vol. 7, no. 1, pp. 51-61.
11. S.K. Parida, B.R. Rout, Free convective flow through porous medium with variable permeability in slip flow regime with couple stress in the presence of heat source, 2017, Journal of Engineering Thermophysics, vol. 26, no. 1, pp. 125-138.
12. I. Muhaimin, R. Kandasamy, A.B. Khamis, R. Roslan, Effect of thermophoresis particle deposition chemical reaction on unsteady MHD mixed convective flow over a porous wedge in the presence of temperature-dependent viscosity, 2013, Nuclear Engineering and Design, vol. 261, pp. 95-106.
13. R. Chen, On the analytic solution of MHD flow and heat transfer for two types of viscoelastic fluid over a stretching sheet with energy dissipation, internal heat source and thermal radiation, 2010, International Journal of Heat and Mass Transfer, vol. 53, pp. 4264-4273.
14. M.K. Nayak, G.C. Dash, L.P. Singh, Steady MHD flow and heat transfer of a third grade fluid in wire coating analysis with temperature dependent viscosity, 2014, International Journal of Heat and Mass Transfer, vol. 79, pp. 1087-1095.

15. Parida. S.K, M.R. Acharya, G.C. Dash, S. Panda, MHD flow past a rotating porous plate through porous medium rotating about a non coincident parallel axis, 2011, AMSE Journals, Series: Modeling, Measurement and Control B, Vol. 80, no. 1-2, pp. 88-103.
16. Parida. S.K. and Dash G.C. Mass transfer and free convective elastico-viscous dusty fluid past through a vertical porous plate in presence of heat source, 2013, AMSE Journals, Series Modelling, Measurement and Control B, Vol. 82 (2), pp. 1-17.
17. Panda. J.P., Dash. N. and Dash. G.C. Three dimensional MHD free convective flow with heat and mass transfer through a porous medium with periodic permeability, 2011, AMSE Journals, Series: Modelling B, Vol. 80 (1), pp.1-17.
18. Sahoo. S.N., Panda J.P. and Dash. G.C. Unsteady two dimensional MHD flow and heat transfer of an elastico-viscous liquid past an infinite hot vertical porous surface bounded by porous medium with source/sink, 2011, AMSE Journals, Series: Modelling B; Vol-80, No.2, pp. 26-42.
19. J.P. Panda, N. Dash, Dash. G.C., Hydro-magnetic flow and heat transfer through porous medium in a elastico-viscous fluid over a porous plate in the slip flow regime, 2011, AMSE Journals, series Modelling B, Vol.80, no. 2, pp.88-101.
19. M.M. Rahman, Locally similar solutions for hydromagnetic and thermal slip flow boundary layers over a flat plate with variable fluid properties and convective surface boundary condition, 2011, Mechanica, vol. 46, no. 5, pp. 1127–1143.
20. M.F. El-Sayed, N.S. Elgazery, Effect of variations in viscosity and thermal diffusivity on MHD heat and mass transfer flow over a porous inclined radiate plane, 2011, Eur. Phys. J. Plus, vol. 126, p. 124.
21. P.R. Sharma, G. Singh, Effects of variable thermal conductivity and heat source/sink on a MHD flow near a stagnation point on a linearly stretching sheet, 2009, Journal of Applied Fluid Mechanics, vol. 2, no. 1, pp. 13-21.
22. L. Talbot, R.K. Cheng, R.W. Schefer, D.R. Willis, Thermophoresis of particles in a heated boundary layer, 1980, Journal of fluid Mechanics, vol. 101, no. 4, pp. 737-758.
23. G.K. Batchelor, C.J. Shen, Thermophoretic deposition of particles in gas flows over cold surface, 1985, Colloid Interface Sci., vol. 107, no. 1, pp. 21-37.
24. E.M. Sparrow, W.J. Minkowycz, E.R.G. Eckert, J. Heat Transfer, Vol. 86 C, p. 508.
25. H. Schlichting, K. Gersten, Boundary Layer Theory, Springer, 8th Edition pp. 313- 314
26. J.X. Ling, A. Dybbs, Forced convection over a flat plate submersed in a porous medium; variable viscosity case, 1987, ASME, New York, 87-WA/HT-23.

27. M. Arunachalam, N.R. Rajappa, Forced convection in liquid metals with variable thermal conductivity and capacity, 1978, Acta Mechanica, vol. 31, pp. 25-31.
28. T.C. Chaim, Heat transfer in a fluid with variable thermal conductivity over stretching sheet, 1998, Acta Mechanica, vol. 129, pp. 63-72.
29. S.R. Pop, T. Grosan, I. Pop, Radiation effect on the flow near the stagnation point of a stretching sheet, 2004, Technische Mechanik, vol. 25, pp. 100-106.
30. T.R. Mahapatra, A.S. Gupta, Heat transfer in a stagnation point flow towards a stretching sheet, 2002, Heat and Mass Transfer, vol. 38, pp. 517-521.

Nomenclature

u, v x- and y-components of the velocity field

x , y cartesian co-ordinates along x-,y- axes respectively

B_0 magnetic field intensity

ε thermal conductivity parameter

μ dynamic viscosity

T_w temperature at the surface of the plate

T_f reference temperature

T temperature of the fluid within the boundary layer

T_∞ temperature of the ambient fluid

$U(x)$ free stream velocity

μ_∞ dynamic viscosity at ambient temperature

ν kinematic viscosity

σ electrical conductivity

λ ratio of free stream velocity to stretching sheet

ψ stream function

η similarity variable

θ dimensionless temperature

ϕ dimensionless concentration

θ_r variable viscosity parameter

Re_x local Reynolds number

ρ fluid density

k thermal conductivity

k_∞ thermal conductivity at ambient temperature

Pr Prandtl number

C_p specific heat at constant pressure

h_w convective heat transfer coefficient

a, b constant stretching rates

f dimensionless stream function

M Hartmann number

S local heat source/sink parameter

C_f local skin-friction coefficient

Nu local Nusselt number

Sh local Sherwood number

Sc Schmidt number

Nc concentration difference parameter

τ thermophoretic parameter

q_w rate of heat transfer

q_m rate of mass transfer

Q volumetric rate of heat generation/absorption

Kp porosity parameter

$u_w(x)$ velocity of stretching sheet

τ_w shear stress

Subscripts

w, ∞ surface condition; ambient condition